Articles

Bis[η^5-tetramethyl(trimethylsilyl)cyclopentadienyl]titanium(II) and Its π-Complexes with Bis(trimethylsilyl)acetylene and Ethylene

Michal Horáček,[†] Volkmar Kupfer,[‡] Ulf Thewalt,[‡] Petr Štěpnička,[§] Miroslav Polášek,[†] and Karel Mach*,[†]

J. Heyrovský Institute of Physical Chemistry, Academy of Sciences of the Czech Republic, Dolejškova 3, 182 23 Prague 8, Czech Republic, Sektion für Röntgen- und Elektronenbeugung, Universität Ulm, 89069 Ulm, Germany, and Department of Inorganic Chemistry, Charles University, Hlavova 2030, 128 40 Prague 2, Czech Republic

Received April 21, 1999

Thermally induced elimination of bis(trimethylsilyl)acetylene from its titanocene complex [{η^5-$C_5Me_4(SiMe_3)$}$_2$Ti(η^2-$Me_3SiC{\equiv}CSiMe_3$)] (**1**) afforded the stable titanocene [{η^5-$C_5Me_4(SiMe_3)$}$_2$Ti^{II}] (**2**) in high yield under mild conditions. Compound **2** exhibits paramagnetic line broadening of ^{1}H NMR signals, although it is silent in EPR spectra down to −196 °C. The solid-state structure determination revealed an exactly parallel arrangement of the cyclopentadienyl rings in **2** due to crystallographically imposed symmetry. Complex **2** smoothly reacts with ethylene to give the yellow η^2-ethylene complex [{η^5-$C_5Me_4(SiMe_3)$}$_2$-Ti(η^2-$CH_2{=}CH_2$)] (**3**). The structures of **1** and **3**, determined by single-crystal X-ray diffraction, show the bent-titanocene moieties with the η^2-coordinated $Me_3SiC{\equiv}CSiMe_3$ and $CH_2{=}CH_2$ ligands, respectively.

Introduction

Metallocenes [(η^5-C_5R_5)$_2$M] and their derivatives are undoubtedly a milestone in the development of transition-metal organometallic chemistry, affording evidence on the diverse properties of metal−cyclopentadienyl ring bonds. In the class of electron-deficient early transition metals (Ti, Zr, Hf; Nb, Ta; Mo, W), however, such data are mostly available only indirectly from metallocene derivatives. The respective metallocenes are highly unstable, since they tend tenaciously to stabilize themselves by acquiring other ligands or by forming new bonds through various rearrangements in order to increase the number of valence electrons.[1] Among these metallocenes, much effort has been devoted to obtaining titanocene, [(η^5-C_5H_5)Ti^{II}], as it remains the last unknown metallocene in the 3d series transition metals. All attempts to reduce the starting material titanocene dichloride have led in most cases to the bright green dimeric titanocene [{(η^5-C_5H_5)Ti}$_2$(μ-η^5:η^5-$C_{10}H_8$)(μ-H)$_2$],[2] to the dimeric hydride complex [{(η^5-C_5H_5)$_2$Ti}$_2$-(μ-H)$_2$],[3] or to titanocene complexes with electron donors capable of π-back-bonding [(η^5-C_5H_5)$_2$TiL$_2$], where L$_2$ = $(PF_3)_2$,[4] $(PMe_3)_2$,[5] $(CO)_2$,[6] $Me_2P(CH_2)_2PMe_2$,[7] and $R_1C{\equiv}CR_2$ ($R_1 = R_2 = Ph$;[8a] $R_1 = Ph$, $R_2 = SiMe_3$;[8b] $R_1 = R_2 = SiMe_3$[8c,d]). Replacement of protons on the cyclopentadienyl (Cp) rings by methyl groups stabilizes electron-deficient metallocenes by steric shielding as well as by increasing electron density on the metal due to the increased electron-donating ability of the Cp ligand. Indeed, permethyltitanocene, [(η^5-C_5Me_5)$_2$Ti^{II}], was first obtained by elimination of nitrogen from the [{(η^5-C_5Me_5)$_2$Ti}$_2$(μ-N_2)] complex, although it was contaminated by the hydride species [(η^5-C_5Me_5)(η^1:η^5-$C_5Me_4CH_2$)TiH],

* To whom correspondence should be addressed. E-mail: mach@jh-inst.cas.cz.
† Academy of Sciences of the Czech Republic.
‡ Universität Ulm.
§ Charles University.

(1) (a) Long, N. J. *Metallocenes*; Blackwell Science: Oxford, U.K., 1998. (b) Beckhaus, R. In *Metallocenes*; Togni, A., Halterman, R. L., Eds.; Wiley-VCH: Weinheim, Germany, 1998; Chapter 4, pp 153−239.
(2) (a) Brintzinger, H. H.; Bercaw, J. E. *J. Am. Chem. Soc.* **1970,** *92,* 6182−6185. (b) Troyanov, S. I.; Antropiusová, H.; Mach, K. *J. Organomet. Chem.* **1992,** *427,* 49−55 and references therein.
(3) (a) Bercaw, J. E.; Brintzinger, H. H. *J. Am. Chem. Soc.* **1969**, *91,* 7301−7306. (b) Bercaw J. E.; Marvich, R. H.; Bell, L. G.; Brintzinger, H. H. *J. Am. Chem. Soc.* **1972**, *94*, 1219−1238.
(4) Sikora, D. J.; Rausch, M. D.; Rogers, R. D.; Atwood, J. L. *J. Am. Chem. Soc.* **1981**, *103*, 1265−1267.
(5) Kool, L. B.; Rausch, M. D.; Alt, H. G.; Herberhold, M.; Thewalt, U.; Honold, B. *J. Organomet. Chem.* **1986**, *310*, 27−34 and references therein.
(6) Sikora, D. J.; Macomber, D. W.; Rausch, M. D. *Adv. Organomet. Chem.* **1986**, *25*, 317−379.
(7) Girolami, G. S.; Wilkinson, G.; Thorntonpett, M.; Hursthouse, M. B. *J. Chem. Soc., Dalton Trans.* **1984**, 2347−2350.
(8) (a) Shur, V. B.; Burlakov, V. V.; Vol'pin, M. E. *J. Organomet. Chem.* **1988**, *347*, 77−83. (b) Rosenthal, U.; Görls, H.; Burlakov, V. V.; Shur, V. B.; Vol'pin, M. E. *J. Organomet. Chem.* **1992**, *426*, C53−C57. (c) Burlakov, V. V.; Rosenthal, U.; Petrovskii, P. V.; Shur, V. B.; Vol'pin, M. E. *Metalloorg. Khim.* **1988**, *1*, 953−954. (d) Burlakov, V. V.; Polyakov, A. V.; Yanovsky, A. I.; Struchkov, Yu. T.; Shur, V. B.; Vol'pin, M. E.; Rosenthal, U.; Görls, H. *J. Organomet. Chem.* **1994**, *476*, 197−205.

10.1021/om990286k CCC: $18.00
Publication on Web 08/08/1999

Scheme 1

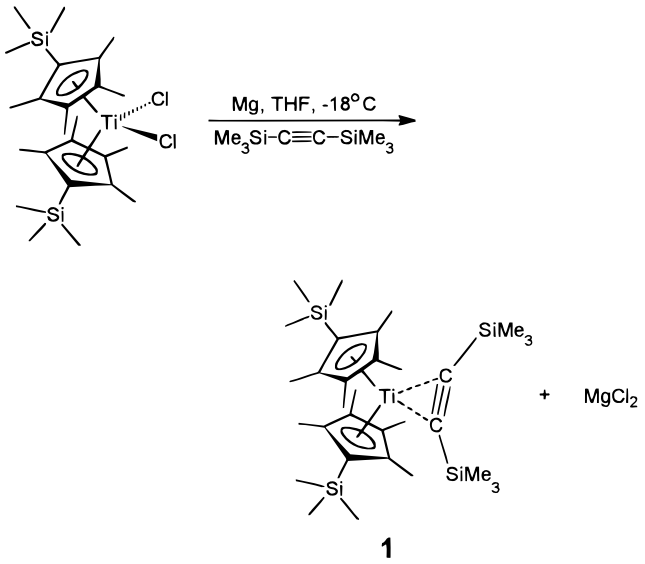

an inherent product of rearrangement.[9] Octamethyltitanocene prepared in an analogous way decomposes rapidly by a hydrogen elimination, affording the dimeric complex [{(η^5-C_5HMe_4)Ti(μ-η^5:η^1-C_5Me_4)}$_2$].[10] Neither of the aforementioned titanocenes was obtained in a crystalline form.

A successful synthesis of a crystalline titanocene was reported very recently: bis[η^5-(*tert*-butyldimethylsilyl)-tetramethylcyclopentadienyl]titanium(II) was obtained from the reduction of [{η^5-C_5Me_4($SiMe_2$-*t*-Bu)}$_2$TiCl] by sodium amalgam in toluene.[11] Independently, we have developed an efficient alternative method for the synthesis of analogous titanocenes and applied it toward the synthesis of the trimethylsilyl derivative.[12] Here we describe the synthesis, spectral characterization, and crystal structures of [{η^5-C_5Me_4($SiMe_3$)}$_2$$Ti^{II}$] (**2**), its precursor [{η^5-C_5Me_4($SiMe_3$)}$_2$Ti(η^2-$Me_3SiC{\equiv}CSiMe_3$)] (**1**), and its complex with ethylene [{η^5-C_5Me_4($SiMe_3$)}$_2$-Ti(η^2-$CH_2{=}CH_2$)] (**3**).

Results and Discussion

The starting complex **1** was obtained by the reduction of the titanocene dichloride [{η^5-C_5Me_4($SiMe_3$)}$_2$$TiCl_2$][13] with activated magnesium in THF in the presence of a large excess of bis(trimethylsilyl)acetylene (BTMSA) at −18 °C (Scheme 1). At elevated temperature (60 °C), which is commonly used in the synthesis of the nonsilylated analogues of **1**, [(η^5-$C_5H_{5-n}Me_n$)$_2$Ti(η^2-$Me_3SiC{\equiv}CSiMe_3$)] (n = 0−5),[8d,14] the paramagnetic complexes

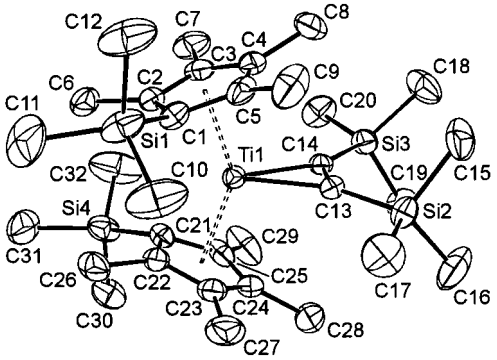

Figure 1. ORTEP drawing of **1** with 30% probability thermal ellipsoids and the atom-numbering scheme. For clarity, all hydrogen atoms are omitted.

Scheme 2

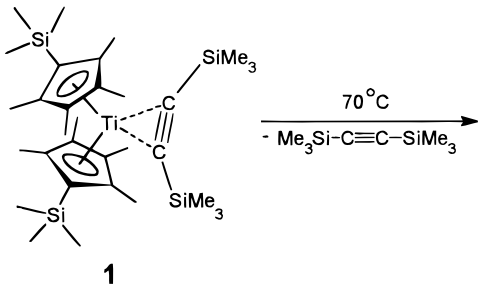

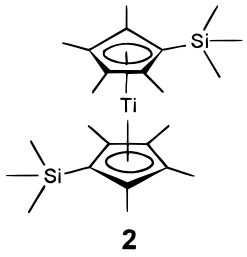

[{η^5:η^1-C_5Me_4($SiMe_2CH_2$)}{η^5-C_5Me_4($SiMe_3$)}Ti^{III}] (**4**) and [{{η^5-$C_5Me_4SiMe_2$(μ-CH_2(Mg,Mg))}{η^5-C_5Me_4($SiMe_3$)}-Ti^{III}(μ-H)$_2$Mg(THF)}$_2$] (**5**) are obtained instead as the major and the minor products, respectively.[15] To avoid the formation of these and some other byproducts, complex **1**, resulting in the form of a THF/BTMSA solution by the low-temperature reduction, has to be separated from excess magnesium at low temperature, as well. Subsequent evaporation of the solvent under vacuum, extraction of the residue by hexane, and crystallization at low temperature affords yellow crystalline **1** in good yield. The compound shows spectroscopic features typical of titanocene−BTMSA complexes, e.g., a large downfield shift of NMR signals due to the coordinated triple bond (δ_C 246.4 ppm), a shift of ν(C≡C) wavenumber to 1600 cm^{-1}, and an electronic absorption band at 980 nm.[14,16] The molecular structure of **1** was verified by single-crystal X-ray diffraction (Figure 1), and its gross features differ only marginally from that of [(η^5-C_5Me_5)$_2$Ti(η^2-BTMSA)] (see below). This contrasts with a remarkably lower thermal stability of **1** compared to that of the latter complex. Whereas [(η^5-C_5Me_5)$_2$Ti(η^2-BTMSA)] thermolyzes at 130 °C,[14] crystal-

(9) (a) Bercaw, J. E.; Brintzinger, H. H. *J. Am. Chem. Soc.* **1971**, *93*, 2045−2046. (b) Bercaw, J. E. *J. Am. Chem. Soc.* **1974**, *96*, 5087−5095.

(10) De Wolf, J. M.; Blaauw, R.; Meetsma, A.; Teuben, J. H.; Gyepes, R.; Varga, V.; Mach, K.; Veldman, N.; Spek, A. L. *Organometallics* **1996**, *15*, 4977−4983.

(11) Hitchcock, P. B.; Kerton, F. M.; Lawless, G. A. *J. Am. Chem. Soc.* **1998**, *120*, 10264−10265.

(12) The synthesis and structure of **2** has already been communicated: Mach, K.; Horáček, M.; Kupfer, V.; Thewalt, U. XXIth Polish-German Colloquy on Organometallic Chemistry; Hotel Star-Dadaj, Poland, September 1998; Book of Abstracts, p 2.

(13) Horáček, M.; Gyepes, R.; Císařová, I.; Polášek, M.; Varga, V.; Mach, K. *Collect. Czech. Chem. Commun.* **1996**, *61*, 1307−1320.

(14) Varga, V.; Mach, K.; Polášek, M.; Sedmera, P.; Hiller, J.; Thewalt, U.; Troyanov, S. I. *J. Organomet. Chem.* **1996**, *506*, 241−251.

(15) Horáček, M.; Hiller. J.; Thewalt, U.; Polášek, M.; Mach, K. *Organometallics* **1997**, *16*, 4185−4191.

(16) Varga, V.; Hiller, J.; Polášek, M.; Sedmera, P.; Thewalt, U.; Mach, K. *J. Organomet. Chem.* **1997**, *538*, 63−74.

line **1** liberates BTMSA upon warming to 70 °C under high vacuum, leaving **2** as a pale green liquid which solidifies upon cooling to room temperature (Scheme 2). The complete removal of BTMSA from **1** can be achieved even at room temperature by repeated dissolving of the solid **1** in hexane and subsequent evaporation of all volatiles under high vacuum. This points to a dissociation equilibrium (eq 1) taking place in solution. Accordingly, the presence of a small amount of noncoordinated BTMSA was detected by NMR spectroscopy in a C_6D_6 solution prepared from crystalline **1**. On the other hand, crystalline **1** is stable under a dynamic vacuum of 10^{-2} Torr at ambient temperature but its EI-MS spectrum shows fragmentation patterns attributable to titanocene **2** and to free BTMSA. The absence of the molecular peak $\mathbf{1}^{\bullet+}$ in the spectrum indicates that **1** dissociates either upon evaporation in the probe or after the electron impact.

$$\mathbf{1} \rightleftarrows \mathbf{2} + \text{BTMSA} \qquad (1)$$

Crude compound **2** obtained by the thermolysis or solvolysis of **1** requires a recrystallization from hexane to remove a more soluble blue paramagnetic impurity.[17] The fact that approximately the same content of the impurity was detected in compound **2** obtained by repeated evaporation of a solution of **1** in hexane at room temperature or by thermolysis of crystalline **1** at 70 °C indicates a good thermal stability of **2**. However, all attempts to purify crude **2** by high-vacuum sublimation at 110 °C failed, affording a product containing a considerably increased amount of the impurity.[17] After crystallization from hexane, pure **2** was obtained as large brown-pink plates which are highly soluble in hexane, benzene-d_6, or toluene to dichroic solutions (the solutions are pale green in incident but red in transmitted light). The electronic absorption spectrum of **2** shows an intense band at 570 nm with a low-intensity shoulder extending to 900 nm. The titanium(II) complex **2** is paramagnetic. Its ^{1}H NMR spectrum consists of two broad signals whose chemical shifts are temperature-dependent, obeying the Curie law in the range observed (0−60 °C). A very similar behavior was reported for the signal of methyl groups in [(η^2-C_5Me_5)$_2$Ti].[9] However, the presence of the spin-unpaired d^2 electrons was not observed in the ESR spectra in the temperature range −196 to +25 °C, probably due to short relaxation times of the spin states. The infrared spectrum of **2** in a KBr pellet shows the bands typical of the $C_5Me_4(SiMe_3)$ ligand, virtually independent of the presence of other coordinated ligands such as (σ-Cl)$_2$, σ-Cl,[13] η^2-C_2H_4, and η^2-BTMSA (see Experimental Section).

Compound **2** in hexane solution does not visually react with gaseous nitrogen at atmospheric pressure in the temperature range −196 to +25 °C. This is at variance with the behavior of [(η^5-C_5Me_5)$_2$Ti][9] and [(η^5-C_5HMe_4)$_2$Ti]],[10] which react reversibly with N_2 to give [{(η^5-C_5Me_5)$_2$Ti}$_2$(μ-N_2)] and [{(η^5-C_5HMe_4)$_2$Ti}$_2$(μ-N_2)], respectively, both displaying an intense blue color. Nevertheless, titanocene **2** reacts smoothly with gaseous ethylene, changing its pale green color to intense yellow. The product of the reaction, [{η^5-$C_5Me_4(SiMe_3)$}$_2$Ti(η^2-CH_2═CH_2)] (**3**), crystallizes from hexane solution as yellow prisms, and its structure was confirmed by X-ray diffraction analysis (see below). The NMR spectra of **3** exhibit features due to the $C_5Me_4(SiMe_3)$ ligand similar to those of **1** and also the resonances of an η^2-coordinated ethylene molecule (δ_H 2.34, δ_C 104.3), which compare well to those reported for [(η^5-C_5Me_5)$_2$Ti(η^2-CH_2═CH_2)] (δ_H 2.02, δ_C 105.1).[18] The electronic absorption spectrum of **3** is nearly identical with the spectrum of **1**, proving that both BTMSA and ethylene ligands are involved in the bonding by one pair of multiple-bond π-electrons, whereas titanium d^2 electrons are donated into the empty π^* orbitals of the ligands.[19]

Table 1. Selected Bond Distances (Å), Bond Angles (deg), and Dihedral Angles (deg) for 1−3, 1*, and 3*

	1	**1***	**2**	**3**	**3***
Ti−C_{av}	2.45(3)	2.43(2)	2.35(3)	2.45(5)	2.41(4)
Ti−CE[a]	2.137(4)[b]	2.114(4)[b]	2.020(2)	2.129(3)	2.092(5)
Ti−C13	2.125(3)	2.122(3)		2.167(4)	2.160(4)
Ti−C14	2.144(3)	2.126(3)			
C13−C14	1.313(4)	1.309(4)		1.442(9)[c]	1.438(5)[c]
CE−Ti−CE′	142.2(1)	138.6(1)	180	147.0(1)	143.6(4)
ϕ[d]	41.4(1)	41.1(1)	0	39.7(1)	40.6(4)

[a] CE denotes the centroid of the corresponding Cp ring. [b] Average value. [c] C13−C13′. [d] Dihedral angle between the least-squares planes of the Cp rings.

Crystal Structures of Compounds 1−3. The crystal structures of compounds **1**−**3** do not represent new structural types, since the structures of [(η^5-C_5Me_5)$_2$Ti-(η^2-BTMSA)] (**1***)[8d] and [(η^5-C_5Me_5)$_2$Ti(η^2-CH_2═CH_2)] (**3***),[18] the permethylated analogues of **1** and **3**, are known. Moreover, the structure of **2** is very similar to that of [{η^5-$C_5Me_4(SiMe_2$-*t*-Bu)}$_2$Ti] (**2′**). Nevertheless, structural data for complexes **1**−**3** and **1*** and **3*** (Table 1) allow us to compare molecular geometry of the parent titanocene with those of its η^2-complexes and to rationalize the significantly higher thermal stability of the silylated titanocenes **2** and **2′** with respect to that of [(η^5-C_5Me_5)$_2$Ti].

The structure of the bent-titanocene complex **1** is asymmetrical (Figure 1), although **1*** exhibits only marginal asymmetry[8d] and the titanium atom of [(η^5-C_5HMe_4)$_2$Ti(η^2-BTMSA)] resides on a crystallographic 2-fold axis.[14] In **1**, a substantial difference in the Ti−C_{alkyne} bond lengths (0.02 Å) is noticeable (Table 1). However, it may originate from solid-state effects and be of no relevance to an intramolecular congestion. The $SiMe_3$ groups on the Cp rings are situated in side positions and do not affect the hindrance between Cp ligands at their hinge position. Consequently, the dihedral angles between the Cp-ring least-squares planes (ϕ) in **1** and **1*** are virtually the same (41.4(1)° vs 41.1(1)°). The presence of the $SiMe_3$ groups has a noticeable effect on the Ti−C(Cp) bond lengths. The average Ti−CE distance is longer by 0.02 Å, and this also accounts for a larger CE−Ti−CE′ angle (142.2(1)° in **1** vs 138.6(1)° in **1***). The average Ti−C_{alkyne} distance is longer only slightly (by 0.01 Å) in **1**, and the C_{alkyne}−

(17) The impurity is identical with the paramagnetic blue waxy solid which is obtained by repeated sublimation of **1**−**3** under vacuum. EPR (toluene, 23 °C): g = 1.9767, ΔH = 3.0 G, a_{Ti} = 7.6 G. EPR (toluene, −140 °C): g_1 = 1.999, g_2 = 1.980, g_3 = 1.953, g_{av}= 1.977. UV−near-IR (hexane, 23 °C, nm): 585.

(18) Cohen, S. A.; Auburn, P. R.; Bercaw, J. E. *J. Am. Chem. Soc.* **1983**, *105*, 1136−1143.

(19) Stockis, A.; Hoffmann, R. *J. Am. Chem. Soc.* **1980**, *102*, 2952−2962.

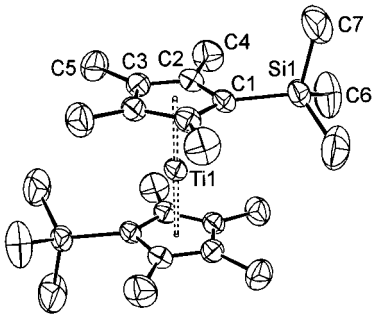

Figure 2. Molecular structure of **2** showing the atom-labeling scheme. Thermal ellipsoids are drawn at the 50% probability level; all hydrogen atoms are omitted for clarity. The nonlabeled atoms are generated by the following symmetry operations: $-x, -y, -z$; $x, -y, -z$; $-x, y, z$.

Table 2. Selected Bond Lengths (Å) and Bond Angles (deg) for 2[a]

Ti(1)−C(1)	2.322(4)	C(2)−C(4)	1.506(4)
Ti(1)−C(2)	2.334(3)	C(3)−C(3)^i	1.399(5)
Ti(1)−C(3)	2.386(3)	C(3)−C(5)	1.501(4)
C(1)−C(2)	1.427(4)	Si(1)−C(6)	1.848(4)
C(1)−Si(1)	1.875(4)	Si(1)−C(7)	1.854(6)
C(2)−C(3)	1.416(4)	Ti(1)−CE(1)	2.020(2)
CE(1)−Ti−CE(2)	180.0	C(3)−C(2)−C(1)	109.3(2)
C(3)^i−C(3)−C(2)	107.97(16)	C(2)−C(1)−C(2)^i	105.6(3)

[a] Symmetry transformation: (*i*) $-x, y, z$.

C_{alkyne} bond lengths are equal within the precision of the measurements.

The crystal structure of **2** is of a higher symmetry (orthorhombic, *Cmca*) than that of **2′** (monoclinic, $P2_1/n$).[11] The titanium atom sits on an inversion center; a mirror plane contains the Ti atom, Si atoms, four carbon atoms, and two hydrogen atoms, and a 2-fold axis perpendicular to the plane passes the Ti atom. The imposed symmetry implies that the Cp rings are exactly planar and parallel, and the normal to these planes contains the Ti atom and both centroids (Figure 2). An inspection of bond distances and bond angles (Table 2) shows that the Cp ring is distorted by the presence of the trimethylsilyl substituent: the C−C bonds involving C(1), the $SiMe_3$-substituted carbon atom, are the longest within the ring C−C bonds, and the C−C−C angle at this carbon atom is the smallest among the ring internal angles. This silicon-induced distortion of the ring also results in different Ti−C(Cp) distances. The carbon atoms of the Cp methyl groups and the Si atom are bent from the ring plane out from the metal center by 0.07 and 0.31 Å, respectively. The molecular parameters of **2** and **2′** are equal to each other within the precision of the measurement, and the reported comparison of Ti−CE distances for **2′** and representative titanocene complexes[11] is fully applicable to **2**.

The molecular structure of **3** (Figure 3) exhibits gross features similar to **1** and closely resembles that of **3***. The comparison of molecular parameters of **3** and **3*** (Table 1) shows that the dihedral angles ϕ are virtually equal in both cases, whereas the Ti−C bond lengths are longer, and consequently, the CE−Ti−CE′ angle is larger in **3**. The C−C bond lengths in π-coordinated ethylene in both **3** and **3*** do not differ.

The comparison of molecular parameters in pairs of compounds **1**, **1***, and **3**, **3*** indicates that the replacement of one methyl group in the permethyltitanocene

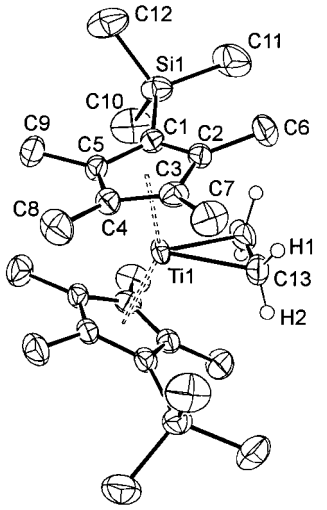

Figure 3. Molecular structure of **3** showing the atom-numbering scheme. Thermal ellipsoids are drawn at the 50% probability level. All hydrogen atoms are omitted, except those of the ethylene ligand. The nonlabeled atoms are generated by the following symmetry operation: $-x, y, -z + 2$.

frame by the $SiMe_3$ group induces a considerable extension of the Ti−C(Cp) bonds and in the case of **1** also an extension of Ti−C_{alkyne} bond length (average 0.01 Å). The ease of liberation of BTMSA from **1** (70 °C), **1*** (130 °C), and [$(C_5HMe_4)_2$Ti(BTMSA)] (200 °C) may be relevant to the Ti−C_{alkyne} bond lengths (average 2.134, average 2.124, and 2.106 Å, respectively).[14] The elongation of Ti−C(Cp) is accompanied by a distortion of the Cp rings that was described in detail for **2**, where no steric congestion, inherent in the bent arrangement, may interfere. Regardless of the stereoelectronic reasons for these effects, the bond extension implies that the hydrogen abstraction by the central titanium atom from the $C_5Me_4(SiMe_3)$ ligands requires a higher activation energy than the hydrogen abstraction from a more closely located C_5Me_5 ligand. In other words, the Ti−C bond extension accounts for a higher stability of **2** and **2′** toward hydride abstraction reactions, yielding, e.g., η^3:η^4-allyldiene[20] or η^1:η^5-fulvene complexes[9a,21] from [$(\eta^5$-$C_5Me_5)_2$Ti]. A significantly shorter Ti−CE distance in **2** in comparison to those in **1** and **3** is apparently brought about by a lower coordination number of the central atom. Provided the extension of Ti−C bonds as found for pairs **1**, **1*** and **3**, **3*** applies to **2** and [$(\eta^5$-$C_5Me_5)_2$Ti], the Ti−CE distance in the latter compound should be very close to 2.00 Å. The reason for the parallel arrangement of the Cp rings in **2** (and **2′**) is to be sought in the crystal-packing effects and a possible small gain of electronic energy in the pseudo D_{5d} configuration of **2**.[22] The interpretation of the parallel structure due to intramolecular crowding of the methyl groups of one ring and the methyl groups of the $SiMe_2$-(*t*-Bu) group of the other Cp ring[11] does not seem to be

(20) Pattiasina, J. W.; Hissink, C. E.; de Boer, J. L.; Meetsma, A.; Teuben, J. H.; Spek, A. L. *J. Am. Chem. Soc.* **1985**, *107*, 7758−7759.
(21) Fischer, J. M.; Piers, W. E.; Young, V. G. *Organometallics* **1996,** *15*, 2410−2412.
(22) Theoretical calculations for early-transition-metal metallocenes by extended Hückel[22a] and ADF methods[22b] assume a negligible energy difference in parallel and bent structures: (a) Lauher, J. W.; Hoffmann, R. *J. Am. Chem. Soc.* **1976**, *98*, 1729−1741. (b) Green, J. C. *Chem. Soc. Rev.* **1998**, 263−271.

justified in view of solid-state structures of **1** and **3**, which show the bending in the direction perpendicular to the Si−Si line with the Si atoms deviated from the least-squares Cp planes by as much as 0.69 and 0.82 Å in **1** and as little as 0.17 Å in **3**.

Concluding Remarks

The preparation of titanocene **2** by thermally induced elimination of the BTMSA ligand from the bent-titanocene complex **1** represents a novel approach toward synthesis of titanocenes, offering an alternative to generally used reduction methods.[23] It also exemplifies the primary step of a dissociative mechanism which has been proposed for various reactions of titanocene−BTMSA complexes with σ-electron donors or acetylenes on the basis of reaction intermediates or products.[24] In contrast, zirconocene−BTMSA complexes react currently by an associative mechanism, probably due to a larger atom diameter and a higher electropositivity of zirconium.[25] On the other hand, these properties may make the preparation and isolation of zirconocene yet more difficult. In the case of **2**, its good thermal stability and inertness toward nitrogen are induced by the $SiMe_3$ substituent at the methylated cyclopentadienyl ligands. The comparison of molecular parameters of a series of compounds related to **2** showed that this can be hardly accounted for by only the steric effects of a bulky silyl group. Subtle electronic effects of the trimethylsilyl group on energies of d-based frontier orbitals are not well understood, although a huge amount of experimental material on the transition-metal silyl compounds is available[26] and theoretical approaches are currently being developed.[27]

Experimental Section

General Considerations. All manipulations, including spectroscopic measurements, were performed under vacuum using all-sealed glass devices equipped with breakable seals. ^1H (399.95 MHz), $^{13}C\{^1H\}$ (100.58 MHz), and ^{29}Si (79.46 MHz) NMR spectra were recorded on a Varian UNITY Inova 400 spectrometer in C_6D_6 solutions at 25 °C. ^{29}Si NMR spectra were measured by the DEPT pulse sequence. Chemical shifts (δ/ppm) are given relative to the solvent signal (δ_H 7.15, δ_C 128.0) and to external tetramethylsilane in C_6D_6 (δ_{Si} 0). EI-MS spectra were obtained on a VG-7070E mass spectrometer at 70 eV. The crystalline samples in sealed capillaries were opened and inserted into the direct inlet under argon. GC-MS analyses were performed on a Hewlett-Packard gas chromatograph (5890 series II) equipped with an SPB-1 capillary column (length 30 m; Supelco) and a mass spectrometric detector (5971 A). EPR spectra were obtained on an ERS-220 spectrometer (Center for Production of Scientific Instruments, Academy of Sciences of GDR, Berlin, Germany) operated by a CU-1 unit (Magnettech, Berlin, Germany) in the X-band. g values were determined by using an Mn^{2+} standard at $g = 1.9860$ ($M_I = -^1/_2$ line). A variable-temperature unit (STT-3) was used for measurements in the range −196 to +25 °C. UV−near-IR spectra in the range 280−2000 nm were measured on a Varian Cary 17D spectrometer in all-sealed quartz cuvettes (Hellma). KBr pellets were prepared in a Labmaster 130 glovebox (mBraun) under purified nitrogen. IR spectra were measured in an air-protecting cuvette on a Specord IR-75 (Carl Zeiss, Jena, Germany) infrared spectrometer.

Chemicals. The solvents THF, hexane, and toluene were dried by refluxing over $LiAlH_4$ and stored as solutions of the dimeric titanocene $[\{(\eta^5\text{-}C_5H_5)Ti\}_2(\mu\text{-}\eta^5\text{:}\eta^5\text{-}C_{10}H_8)(\mu\text{-}H)_2]$.[28] Bis(trimethylsilyl)acetylene (BTMSA, Fluka) was degassed, stored as a solution of dimeric titanocene for 4 h, and distilled into ampules on a vacuum line. Magnesium turnings (Fluka, purum for Grignard reactions) were first used in large excess for the preparation of $[(\eta^5\text{-}C_5Me_5)_2Ti(\eta^2\text{-BTMSA})]$.[14] Then, activated magnesium was separated from the reaction mixture, washed thoroughly with THF, and stored in ampules equipped with breakable seals. Ethylene (polymerization grade; Polymer Institute Brno, Brno, Czech Republic) was condensed at liquid-nitrogen temperature, degassed under high vacuum, and expanded to a reservoir under ambient pressure. The synthesis of $[\{\eta^5\text{-}C_5Me_4(SiMe_3)\}_2TiCl_2]$ was carried out as recently reported.[13]

Preparation of $[\{\eta^5\text{-}C_5Me_4(SiMe_3)\}_2Ti(\eta^2\text{-}Me_3SiC{\equiv}CSiMe_3)]$ (1). The complex $[\{\eta^5\text{-}C_5Me_4(SiMe_3)\}_2TiCl_2]$ (1.0 g, 2.0 mmol) was degassed and rapidly mixed with activated magnesium (ca. 0.5 g, 20 mmol), BTMSA (3.0 mL, 13.4 mmol), and THF (40 mL). The mixture was cooled to −18 °C in a freezer before the solution turned blue, to avoid byproduct formation due to a rapid reduction of $[\{\eta^5\text{-}C_5Me_4(SiMe_3)\}_2TiCl]$. After 40 h at −18 °C with occasional shaking, the resulting yellow solution was rapidly separated from unreacted magnesium while the temperature was kept below −5 °C. THF and BTMSA were distilled off under vacuum, and the residue was extracted by hexane. The yellow hexane solution was allowed to stand overnight at −5 °C, whereupon a white powder (likely $MgCl_2$) separated from a clear yellow solution. The solution was concentrated and cooled to −18 °C overnight to give a crop of **1** as yellow crystals, which were separated from the mother liquor at −5 °C. Yield 1.0 g (80%). The crystals were directly used for X-ray diffraction analysis and all spectroscopic measurements. Recrystallization of this material from hexane afforded a crystalline mixture of **1** and **2**. Data for **1** are as follows. ^1H NMR (C_6D_6): δ −0.07, 0.08 (2 × s, 18H, Me_3Si); 1.89, 2.04 (2 × s, 12H, $C_5(CH_3)_4(Me_3Si)$). $^{13}C\{^1H\}$ NMR (C_6D_6): δ 3.5, 4.8 (Me_3Si); 14.6, 17.5 ($(CH_3)_4(Me_3Si)C_5$); 118.7 (C(Cp)−$SiMe_3$); 129.8, 130.1 (C(Cp)−Me); 246.4 (η^2−$C{\equiv}C$). ^{29}Si NMR (C_6D_6): δ −16.1 (η^2-$(Me_3Si)_2C_2$), −7.5 ($(CH_3)_4(Me_3Si)C_5$). The sample contained a small amount of free BTMSA. IR (KBr, cm^{-1}): 2946 (s), 2887 (s), 1620 (sh), 1595 (s), 1560 (sh), 1453 (m), 1403 (w), 1373 (m), 1333 (w), 1317 (s), 1242 (vs), 1124 (m), 1015 (m), 840 (vs), 752 (s), 677 (m), 652 (w), 633 (m), 618 (w), 447 (m). UV−near-IR (hexane, 22 °C, nm): 980. EI-MS (direct inlet, 70 eV, 60−80 °C): cluster of peaks with the most abundant m/z 434 ($[M - BTMSA]^+$) and peaks arising from BTMSA at m/z 170, 155, and 73 in relative abundances corresponding well to those of free BTMSA. Intensities of the peaks due to BTMSA decreased with respect to those of (M −

(23) Compound **2** can be obtained by the reduction of $[\{\eta^5\text{-}C_5Me_4(SiMe_3)\}_2TiCl_2]$ by active Mg in THF at room temperature, however, it is strongly contaminated by the impurity described in ref 17, by the hydride **5**,[15] or by $[\{\eta^5\text{-}C_5Me_4(SiMe_3)\}_2TiCl]$.[13]

(24) (a) Burlakov, V. V.; Dolgushin, F. M.; Yanovsky, A. I.; Struchkov, Yu. T.; Shur, V. B.; Rosenthal, U.; Thewalt, U. *J. Organomet. Chem.* **1996**, *522*, 241−247. (b) Burlakov, V. V.; Polyakov, A. V.; Yanovsky, A. I.; Struchkov, Yu. T.; Shur, V. B.; Vol'pin, M. E.; Rosenthal, U.; Görls, H. *J. Organomet. Chem.* **1994**, *476*, 197−206. (c) Ohff, A.; Zippel, T.; Arndt, P.; Spannenberg, A.; Kempe, R.; Rosenthal, U. *Organometallics* **1998**, *17*, 4429−4437. (d) Witte, P. T., Klein, R.; Kooijman, H.; Spek, A. L.; Polášek, M.; Varga, V. Mach, K. *J. Organomet. Chem.* **1996**, *519*, 195−204.

(25) (a) Mansel, S.; Thomas, D.; Lefeber, C.; Heller, D.; Kempe, R.; Baumann, W.; Rosenthal, U. *Organometallics* **1997**, *16*, 2886−2890. (b) Thomas, D.; Arndt, P.; Peulecke, N.; Spannenberg, A.; Kempe, R.; Rosenthal, U. *Eur. J. Inorg. Chem.* **1998**, 1351−1357. (c) Zippel, T.; Arndt, P.; Ohff, A.; Spannenberg, A.; Kempe, R.; Rosenthal, U. *Organometallics* **1998**, *17*, 4429−4437.

(26) Corey, J. Y.; Braddock-Wilking, J. *Chem. Rev.* **1999**, *99*, 175−292.

(27) Yoshida, J.; Nishiwaki, K. *J. Chem. Soc., Dalton Trans.* **1998**, 2589−2596.

(28) Antropiusová, H.; Dosedlová, A.; Hanuš, V.; Mach, K. *Transition Met. Chem.* **1981**, *6*, 90−93.

Table 3. Crystallographic Data and Details of the Data Collection and Structure Refinement for 1−3[a]

	1	2	3
formula	$C_{32}H_{60}Si_4Ti$	$C_{24}H_{42}Si_2Ti$	$C_{26}H_{46}Si_2Ti$
M_r	605.06	434.66	462.71
cryst syst	monoclinic	orthorhombic	monoclinic
space group	*I*2/*a* (No. 15)	*Cmca* (No. 64)	*C*2/*c* (No. 15)
a (Å)	18.807(2)	14.087(3)	17.241(5)
b (Å)	18.927(2)	11.574(2)	8.309(2)
c (Å)	21.214(2)	16.137(3)	18.878(5)
β (deg)	97.180(16)		98.65(2)
V (Å^3); *Z*	7492.1(15); 8	2631.1(8); 4	2673.6(12); 4
D_{calcd} (g cm^{-3})	1.073	1.097	1.150
μ (mm^{-1})	0.374	0.423	0.420
color, habit	yellow, prism	brown-pink, prism	yellow, prism
cryst dimens (mm^3)	0.3 × 0.3 × 0.5	0.2 × 0.3 × 0.4	0.2 × 0.3 × 0.3
no. of diffractions collected	13 477	8010	7847
2θ range (deg)	4.30−52.08	5.04−48.2	2.39−24.07
hkl range	−22 to +18; −19 to +23; −18 to +26	−16 to +16; −13 to +13; −18 to +18	−19 to +18; −9 to +8; −21 to +21
no. of unique diffractions	7125	1085	2084
no. of obsd diffractions, $I > 2\sigma(I)$	3059	925	1452
F(000)	2640	944	1008
no. of params	334	68	140
$R(F)$; $R_w(F^2)$ (%)	11.43; 10.63	5.62; 15.23	7.80; 13.09
GOF (F^2), all data	0.730	1.084	1.172
$R(F)$; $R_w(F^2)$ ($I > 2\sigma(I)$)	4.72; 9.24	4.91; 14.70	5.42; 12.29
$R(\sigma)$ (%)	13.98	2.64	5.66
$\Delta\rho$ (e Å^{-3})	0.232; −0.273	0.353; −0.272	0.595; −0.645

[a] $R(F) = \sum||F_o| - |F_c||/\sum|F_o|$, $R_w(F^2) = [\sum(w(F_o^2 - F_c^2)^2)/(\sum w(F_o^2)^2)]^{1/2}$, GOF $= [\sum(w(F_o^2 - F_c^2)^2)/(N_{diffrns} - N_{params})]^{1/2}$, and $R(\sigma) = \sum\sigma(F_o^2)/\sum F_o^2$.

BTMSA) during the course of measurement. Anal. Calcd for $C_{32}H_{60}Si_4Ti$: C, 63.52; H, 9.99. Found: C, 63.56; H, 10.04.

Preparation of [{η^5-$C_5Me_4(SiMe_3)$}$_2$Ti] (2). Crystalline **1** (0.5 g, 0.8 mmol) was heated to 70 °C in a water bath under a vacuum of 10^{-4} Torr while volatiles were collected in a trap cooled by liquid nitrogen. After about 2 h, a pale green liquid remained in the ampule, which solidified upon standing at ambient temperature. GC-MS analysis of the volatiles revealed BTMSA to be the sole component. The solid was dissolved by condensing hexane vapor and crystallized from a minimum amount of hexane at −18 °C to afford **2** as brown-pink platelike crystals. The solutions of **2** in hexane, toluene, or C_6D_6 were pale green.

Alternatively, crystalline **1** was dissolved in fresh hexane, the solution was evaporated under vacuum, and the residue was kept at ambient temperature under dynamic vacuum overnight. Crystallization of the greenish residue from its hexane solution gave the same product as the above procedure. The conversions of **1** to **2** were virtually quantitative. Yields of pure crystals were in both cases ca. 0.2 g (50−60%). The only observable byproduct was an unidentified blue paramagnetic compound.[17] Larger concentrations of this impurity were detected in the mother liquors from the crystallizations. Data for **2** are as follows. ^{1}H NMR (C_6D_6, 25 °C): δ 6.95 (*Me*$_3$Si, $\Delta\nu_{1/2} \approx 40$ Hz), 26.25 ((C*H*$_3$)$_4$(Me$_3$Si)C$_5$), $\Delta\nu_{1/2} \approx 110$ Hz). Chemical shifts follow the Curie law in the range 0−60 °C as proved by numeric regression in the form $\delta = a + bT^{-1}$. IR (KBr, cm^{-1}): 2940 (vs), 2888 (vs), 2850 (vs), 2719 (w), 1473 (m), 1440 (m), 1402 (w), 1372 (m), 1341 (sh), 1327 (s), 1315 (sh), 1241 (vs), 1120 (m), 1080 (w), 1017 (s), 942 (w), 835 (vs), 750 (s), 681 (s), 644 (sh), 629 (s), 613 (m), 573 (s), 555 (sh), 416 (s). UV−near-IR (hexane, 22 °C, nm): 300 > 340 (sh) > 370 (sh) ≫ 570 ≫ 950 (sh). EI-MS (direct inlet, 70 eV, 50−70 °C; *m*/*z* (relative abundance)): 436 (13), 435 (27), 434 ($M^{\bullet+}$, 61), 433 (32), 432 (16), 361 ([M − SiMe$_3$]$^+$, 10), 177 (10), 120 (9), 73 (100). Anal. Calcd for $C_{24}H_{42}Si_2Ti$: C, 66.32; H, 9.74. Found: C, 66.27; H, 9.71.

Preparation of [{η^5-$C_5Me_4(SiMe_3)$}$_2$Ti(η^2-CH_2=CH_2)] (3). On a vacuum line, ethylene at a pressure of 600 Torr was admitted to a solution of **2** (0.2 g, 0.5 mmol) in hexane. The solution was cooled by liquid nitrogen and warmed to room temperature. This cycle was repeated for the second time, although even after the first cycle the pale green solution turned an intense yellow. Ethylene and hexane were evaporated under vacuum, and a yellow crystalline residue was dissolved in hexane. Crystallization from a concentrated solution at −18 °C afforded **3** as greenish yellow crystals. Yield 0.2 g (86%). ^{1}H NMR (C_6D_6): δ −0.08 (s, 9H, *Me*$_3$Si); 1.33 (s, 6H, (C*H*$_3$)$_4$(Me$_3$Si)C$_5$); 2.09 (s, 6H, (C*H*$_3$)$_4$(Me$_3$Si)C$_5$); 2.34 (s, 2H, =C*H*$_2$). ^{13}C{^{1}H} NMR (C_6D_6): δ 2.0 (*Me*$_3$Si); 11.9, 15.6 ((*C*H$_3$)$_4$(Me$_3$Si)C$_5$); 104.3 (=*C*H$_2$); 121.0, 123.8, 130.1 (*C*(Cp)). IR (KBr, cm^{-1}): 2966 (sh), 2948 (vs), 2896 (vs), 2860 (sh), 1650 (w, b), 1476 (m), 1445 (m), 1431 (m), 1372 (m), 1345 (w), 1329 (s), 1244 (vs), 1121 (m), 1080 (w), 1017 (s), 837 (vs), 785 (m), 752 (s), 683 (m), 666 (w), 631 (m), 614 (w), 573 (m), 566 (sh), 553 (sh), 468 (m), 416 (s). UV−near-IR (hexane, nm, 22 °C): 340(sh) ≫ 990 nm. EI-MS (direct inlet, 70 eV, 50−70 °C); *m*/*z* (relative abundance)): a cluster of peaks with the highest abundance of *m*/*z* 433 ([M − C$_2$H$_5$]$^+$, 11), 194 (13), 177 (14), 120 (20), 73 (100). Anal. Calcd for $C_{26}H_{46}Si_2Ti$: C, 67.49; H, 10.02. Found: C, 67.46; H, 9.99.

Attempted Reaction of 2 with Dinitrogen. An evacuated ampule (500 mL) equipped with a glass stopcock and a breakable seal was filled by purified nitrogen to atmospheric pressure in a glovebox and closed. The stopcock was sealed off, and the ampule was attached to another one containing the solution of **2** in hexane. The solution was poured from one ampule to the other with shaking and finally transferred into a device with quartz cuvettes. Neither a visual color change upon cooling the solution to liquid-nitrogen temperature nor any change in its UV−near-IR spectrum on cooling to −15 °C were observed.

X-ray Crystal Determination. Selected crystals of **1**−**3** were mounted in Lindenmann glass capillaries under nitrogen in a glovebox (Labmaster 130, mBraun), and the capillaries were closed with sealing wax. The X-ray measurements were carried out at room temperature on a STOE IPDS imaging plate diffractometer using graphite-monochromated Mo Kα radiation ($\lambda = 0.710\ 73$ Å). The diffraction data were corrected for Lorentz and polarization effects. Since the absorption coefficients were low, no absorption correction was applied. Structures **1** and **3** were solved by direct methods;[29] structure **2** was solved by the heavy-atom (Patterson) method.[30] The refinement was carried out by full-matrix least squares on F^2

(29) Sheldrick, G. M. *Acta Crystallogr.* **1990**, *A46*, 467−473.
(30) Sheldrick, G. M.; Dauter, Z.; Wilson, K. S.; Hope, H.; Sieker, L. C. *Acta Crystallogr.* **1993**, *D49*, 18−23.

using a variance-based weighting scheme in the final stages.[31] All non-hydrogen atoms were refined anisotropically. The hydrogen atoms were included in their calculated positions and readjusted after each refinement cycle. In structure **2**, the hydrogen atoms bonded to C(7) (one H atom by space group symmetry) were identified in a difference Fourier map and then readjusted into their idealized positions. In the structure of **3**, the two hydrogen atoms at C(13) were found on a difference Fourier map and refined isotropically. The relevant crystal data and details on the data collection and the structure refinement for **1**−**3** are given in Table 3.

(31) Sheldrick, G. M. SHELXL97: Program for the Refinement of Crystal Structures; University of Göttingen, Göttingen, Germany, 1997.

Acknowledgment. This research was supported by the Grant Agency of the Academy of Sciences of the Czech Republic (Grant No. A4040711) and by the Volkswagen Stiftung. The Grant Agency of the Czech Republic sponsored access to the Cambridge Structure Database (Grant No. 203/99/0067).

Supporting Information Available: Tables of crystallographic data, atomic coordinates, thermal parameters, intramolecular distances and angles, and dihedral angles of least-squares planes and packing diagrams for **1**−**3**. This material is available free of charge via the Internet at http://pubs.acs.org.

OM990286K